A&A 451, 835–843 (2006)
DOI: 10.1051/0004-6361:20054402


Astronomy & Astrophysics

# Spectroscopy of the brightest optical counterparts of X-ray sources in the direction of M 31 and M 33⋆

D. Hatzidimitriou[1], W. Pietsch[2], Z. Misanovic[2], P. Reig[3], and F. Haberl[2]

[1] University of Crete, Department of Physics, PO Box 2208, 71003 Heraklion, Greece
e-mail: dh@physics.uoc.gr
[2] Max-Planck-Institut für extraterrestrische Physik, 85741 Garching, Germany
[3] IESL, Foundation for Research and Technology, 71110 Heraklion, Greece

Received 24 October 2005 / Accepted 18 January 2006

**ABSTRACT**

*Context.* Recent surveys of the Local Group spiral Galaxies M 31 and M 33 with XMM-Newton yielded a large number of X-ray sources.
*Aims.* As part of the effort to identify and classify the objects responsible for this X-ray emission, we have obtained optical spectra of the brightest optical counterparts of the identified X-ray sources, using the 1.3 m Skinakas Telescope. Most of these objects are foreground star candidates. The purpose of the present study is to confirm this identification and to explore the compatibility between the optical spectral classification and the observed X-ray properties of the sources.
*Methods.* We have obtained optical spectra for the 14 brightest optical counterparts of X-ray sources identified by XMM-Newton in the direction of M 31 and for 21 optical counterparts in the direction of M 33, using the 1.3 m Skinakas telescope in Crete, Greece.
*Results.* All of the M 31 sources and all but one of the M 33 sources were confirmed to be foreground stars, of spectral types between A and M. One of the stars is a late M dwarf with $H_\alpha$ emission, a flare star, also displaying strong X-ray variability. One of the M 33 sources (lying within the D25 ellipse) corresponds to a previously known background galaxy, LEDA 5899.

**Key words.** galaxies: individual: M 31 – galaxies: individual: M 33 – X-rays: galaxies – X-rays: stars – Local Group

## 1. Introduction

Recent surveys of the Local Group spiral Galaxies M 31 (Pietsch et al. 2005a, hereafter PFH2005) and M 33 (Pietsch et al. 2004, hereafter PMH2004) with XMM-Newton yielded a large number of X-ray sources. With their moderate Galactic foreground absorption, both galaxies are ideal for studying the X-ray source population and diffuse emission in nearby spiral galaxies.

The Andromeda galaxy (M 31) is a massive SA(s)b galaxy, located at a distance of 780 kpc (Holland 1998) and seen under an inclination of 78° (de Vaucouleurs et al. 1991).

As described in detail in PFH2005, a total of 856 X-ray sources were detected in an area of 1.24 square degrees. Within M 31, 21 supernova remnants (SNR) and 23 SNR candidates were detected, as well as 18 super-soft source candidates, 7 X-ray binaries and 9 X-ray binary candidates, 27 globular cluster sources and 10 globular cluster source candidates, which most likely are low mass X-ray binaries within the cluster. From 567 hard sources, some are expected to be X-ray binaries or Crab like SNRs within M 31, and the rest, background AGN. As well as the sources within M 31, there were also foreground and background sources: six sources were identified as foreground stars and 90 as foreground star candidates, one as a BL Lac type active galactic nucleus (AGN) and 36 as AGN candidates. One source coincided with the Local Group galaxy M 32, one with a background galaxy cluster and another is a background galaxy cluster candidate.

M 33, an Sc galaxy, is located at a distance of 795 kpc (van den Bergh 1991) and is seen under a relatively low inclination of 56° (Zaritsky et al. 1989). PMH2004 detected a total of 408 sources in a 0.8 square degree field combining the counts of all EPIC instruments. About half of the sources lie within M 33; the rest are background AGNs or foreground stars. Cross-correlation with archival data led to the identification of 5 foreground stars and 30 foreground star candidates, as well as 12 AGN candidates. Within M 33, 21 supernova remnants (SNR) and 23 SNR candidates were identified, as well as 5 super-soft sources and 2 X-ray binaries. From the remaining 267 X-ray sources classified as "hard", those within M 33 may be low or high mass X-ray binaries, or Crab-like SNRs, while a significant fraction of them are expected to be background AGN. Misanovic et al. (2006) analyzed the individual observations of the XMM-Newton data of M 33, detecting 39 new sources and improving the positions of another 311. They also studied the variability of the sources on time scales of hours to months or years, their spectral characteristics and classification. For example, using the detected variability, they were able to classify 8 new X-ray binary candidates.

Pietsch et al. (2005b) searched for X-ray counterparts of optical novae detected in M 31 and M 33 and discovered 21 X-ray counterparts for novae in M 31 – mostly identified as supersoft sources by their hardness ratios – and two in M 33.

As part of the effort of identifying and classifying the objects responsible for the observed X-ray emission in the direction of M 31 and M 33, we have obtained optical spectra of the brightest optical counterparts of the identified X-ray sources, using the 1.3 m Skinakas Telescope. These brightest optical counterparts were taken from PFH2005 for M 31 and from PMH2004 for

⋆ Tables 1 and 2 are also available in electronic form at the CDS via anonymous ftp to cdsarc.u-strasbg.fr (130.79.128.5) or via http://cdsweb.u-strasbg.fr/cgi-bin/qcat?J/A+A/451/835

M 33. Most of these objects are foreground star candidates, as also mentioned in the corresponding reference papers. The purpose of the present study is to confirm this and to explore the compatibility between the optical spectral classification and the observed X-ray properties of the sources. One of the bright optical counterparts that we have observed is the known galaxy LEDA 5899, which was also part of the CFA redshift survey (Huchra et al. 1999).

In the next section, we describe the optical observations; in Sect. 3 we describe the data reduction. In Sect. 4, the method followed for the classification of the spectra obtained is presented and in Sect. 5 we discuss the results, including individual objects of interest.

## 2. Optical observations

The optical observations used in this study were carried out during three observing runs, on September 6, 2003, on October 18–22, 2003 and on October 10–11, 2004, using the 1.3-m Ritchey-Cretien telescope at Skinakas Observatory, located on the island of Crete (Greece).

The telescope was equipped with a 2000x800 ISA SITe CCD camera and a 1302 lines/mm grating, giving a nominal dispersion of 1.04 Å/pixel, and a wavelength coverage from 4748 Å to 6828 Å. The spectral region was selected so as to include both $H_\alpha$ and $H_\beta$ spectral lines. For the three spectra that were obtained in September 2003, the wavelength region was somewhat different, shifted further to the blue (from 3900 Å to 6000 Å). One of these three spectra (of source number 3 in M 33) was also observed in October 2003, with the wavelength coverage used for the bulk of the spectra. As will be discussed later, the two spectra obtained for this object served as a test of the compatibility between the spectral classes obtained in the two different wavelength regions.

Exposure times ranged from 600 to 7200 s, depending on the object's magnitude and on seeing and weather conditions. In most cases, two or more exposures were obtained per object. Each object observation was followed by an arc calibration exposure (CuAr).

A total of 18 standards, of spectral types ranging from O9.5 to M6, were also observed with the same configuration as the targets.

In the first observing run three objects in the direction of M 33 were observed (6/9/2003). In the second run another 19 targets in the direction of M 33 were observed (one of them repeated from the first run, so a total of 21 targets in the direction of M 33 were observed), while in the third, spectra for 14 objects in the direction of M 31 were obtained. The first 6 columns of Table 1 list the details of the observations.

1. Column 1 gives the X-ray source number of the target as it appears in the corresponding X-ray catalogue paper, i.e., in PFH2005 for M 31 and in PMH2004 for M 33. There is one exception, object 3b in the direction of M 33, which was not detected by the automatic procedures due to its far off axis location and thus it was not included in PMH2004 (see Sect. 5.2 for more details).
   For object 122 in the direction of M 33, the bright USNO-B1 star 1210-0020531 given as possible optical counterpart in PMH2004 is actually resolved into two stars on deeper 4m Mosaic images of M 33, separated by ~6″ in the NNE/SSW direction (see Sect. 5.3 for more details). Spectra for both of these stars were obtained.
   If available, Chandra source names are given in the footnotes of the table. For M 31 only one source ([PFH2005] 31) has a Chandra identification, while for M 33 two sources ([PMH2004] 196 and 200) have also been identified in existing Chandra catalogues.
2. Columns 2 and 3 give the co-ordinates of the objects (epoch 2000).
3. Column 4 provides the USNO-B1 identification derived from the cross-correlation between the X-ray catalogue and the USNO-B1 catalogue.
4. Columns 5 and 6 list the $B$ and $R$ magnitudes of the corresponding USNO object (B2 and R2 in the USNO-B1 catalogue). The limiting magnitude of the sample of stars observed in M 33 was $R = 14.75$, while in M 31 it was 12.43. In neither case is the sample of objects observed complete to the corresponding limiting magnitude. The brighter limiting magnitude for the M 31 stars was dictated by observing time limitations only (as three of the nights allocated were lost to poor weather conditions).
5. Column 7 gives the 2MASS identification derived from the cross-correlation between the X-ray catalogue and the 2MASS catalogue.
6. Column 8 provides the corresponding $J$ magnitude of the 2MASS counterpart (as given in the 2MASS catalogue).
7. Column 9 gives the date of the Skinakas observation.
8. Column 10 lists the total exposure time for the specific spectrum, while the number of exposures taken for that object is provided in the parenthesis following the total exposure time.

Figure 1 illustrates how well the X-ray positions correlate with the coordinates of the optical counterparts observed.

## 3. Data reduction

The data reduction was performed using the *STARLINK* Figaro package (Shortridge et al. 2001). The frames were bias subtracted, flat fielded and corrected for cosmic ray events. The 2-D spectra were subsequently sky subtracted using the *POLYSKY* command. A spatial profile was then determined for each 2-D spectrum, and the object spectra were optimally extracted using the algorithm of Horne (1986), with the *OPTEXTRACT* routine. Arc spectra were then extracted from the arc exposures, using exactly the same profiles as for the corresponding object spectra. The arc spectra were subsequently used to calibrate the object spectra. After calibration, spectra from individual exposures of the same object were co-added to yield the final spectrum.

This procedure was followed for almost all of the observations, with one exception, namely object USNO-B1 1210-0020531 in the M 33 list. In this case, a second object was located very close to the target (see Sect. 5.2). The resulting spectra could not be extracted separately using the optimal extraction procedure described above. Due to the slight curvature of the spectra, single linear extraction along the lines of the CCD was not possible either. Thus we have used a step extraction with sufficient wavelength overlap between subsequent extractions to ensure compatibility of the fluxes. The calibrating arc spectra were created in exactly the same way.

The signal-to-noise ratio (S/N) of the final spectra varied from 20 to about 350, with an average of 150.

The same reduction and calibration procedures were followed for the 18 spectroscopic standard stars. Most of the

**Table 1.** Log of objects observed in the direction of M 31 and M 33 and derived spectral types.

| ID* | RA (2000) | Dec (2000) | USNO-B1 ID | *B* | *R* | 2MASS ID | *J* (mag) | Date | Exp. (s) | Spectral type |
|---|---|---|---|---|---|---|---|---|---|---|
| | | | | | M 31 | | | | | |
| 26 | 00 39 43.54 | 40 39 42.1 | 1306-0011237 | 13.00 | 12.43 | 00394351+4039425 | 11.57 | 11/10/04 | 3600 (2) | G0 |
| 31[1] | 00 39 56.53 | 40 41 00.2 | 1306-0011322 | 10.76 | 10.31 | 00395652+4041003 | 9.78 | 10/10/04 | 1200 (2) | F0 |
| 49 | 00 40 13.79 | 40 35 33.9 | 1305-0011683 | 11.74 | 11.46 | 00401383+4035322 | 10.69 | 11/10/04 | 2400 (2) | F5 |
| 59 | 00 40 23.75 | 40 53 06.3 | 1308-0012001 | 10.84 | 10.21 | 00402380+4053069 | 9.70 | 10/10/04 | 1200 (2) | F5 |
| 101 | 00 40 57.11 | 40 56 38.1 | 1309-0012722 | 12.00 | 11.42 | 00405703+4056384 | 10.81 | 11/10/04 | 2400 (2) | F5 |
| 137 | 00 41 24.35 | 40 55 34.6 | 1309-0012839 | 12.34 | 11.49 | 00412410+4055333 | 12.09 | 11/10/04 | 2400 (2) | G8 |
| 168 | 00 41 43.39 | 41 05 06.0 | 1310-0013030 | 11.91 | 11.17 | 00414345+4105047 | 10.35 | 11/10/04 | 2400 (2) | G0 |
| 217 | 00 42 08.89 | 41 23 31.3 | 1313-0012724 | 11.06 | 9.78 | 00420901+4123306 | 8.38 | 10/10/04 | 1200 (2) | G8 |
| 464 | 00 43 32.68 | 41 09 11.1 | 1311-0013521 | 11.58 | 9.96 | 00433260+4109092 | 8.62 | 10/10/04 | 1800 (2) | K0 |
| 479 | 00 43 41.46 | 41 42 24.0 | 1317-0014537 | 11.24 | 10.27 | 00433892+4138472 | 15.58 | 10/10/04 | 1200 (2) | G8 |
| 498 | 00 43 50.31 | 41 24 11.4 | 1314-0013364 | 11.48 | 10.92 | 00435017+4124115 | 10.58 | 10/10/04 | 2400 (2) | F7 |
| 553 | 00 44 23.91 | 42 00 10.1 | 1320-0014047 | 11.51 | 10.70 | 00442392+4200095 | 10.21 | 10/10/04 | 1200 (1) | G0 |
| 615 | 00 45 07.61 | 41 53 57.2 | 1318-0015195 | 12.64 | 11.95 | 00450752+4153581 | 10.22 | 11/10/04 | 2400 (2) | G9 |
| 733 | 00 46 19.32 | 42 21 29.4 | 1323-0017450 | 12.20 | 12.16 | 00461905+4221308 | 10.53 | 11/10/04 | 2400 (2) | G0 |
| | | | | | M 33 | | | | | |
| 3[2] | 01 31 54.90 | 30 29 54.5 | 1204-0019506 | 12.37 | 11.34 | 01315500+3029522 | 9.73 | 06/09/03 | 2700 (2) | G9 |
| | | | | | | | | 18/10/03 | 600 (1) | |
| 3b[3] | 01 31 52.62 | 30 29 26.2 | 1204-0019500 | 17.46 | 14.66 | | | 18/10/03 | 2400 (2) | M3 |
| 28 | 01 32 23.37 | 30 47 48.8 | 1207-0019732 | 14.24 | 11.65 | | | 20/10/03 | 1800 (3) | G9 |
| 39[4] | 01 32 30.25 | 30 36 17.3 | 1206-0019336 | 16.61 | 14.75 | 01323043+3036186 | 13.32 | 20/10/03 | 4800 (3) | K3:: |
| 54 | 01 32 38.67 | 30 12 19.2 | 1202-0019688 | 13.40 | 10.99 | 01323878+3012167 | 11.34 | 20/10/03 | 1200 (2) | G4 |
| 77 | 01 32 51.27 | 30 08 13.2 | 1201-0020193 | 12.55 | 10.89 | 01325128+3008140 | 11.23 | 20/10/03 | 1800 (3) | F5 |
| 92 | 01 32 56.75 | 30 15 44.2 | 1202-0019784 | 10.85 | 9.50 | 01325685+3015429 | 8.20 | 20/10/03 | 600 (1) | G7 |
| | | | | | | | | 21/10/03 | 1200 (2) | |
| 122[5] | 01 33 13.12 | 31 02 52.1 | 1210-0020531 | 15.61 | 13.84 | 01331353+3102527 | 14.58 | | | |
| | 01 33 13.41 | 31 02 48.9 | | | | | | 21/10/03 | 1800 (1) | G0 |
| | 01 33 13.63 | 31 02 52.9 | | | | | | 21/10/03 | 1800 (1) | G5:: |
| 142 | 01 33 22.95 | 30 56 55.0 | 1209-0020773 | 9.45 | 9.04 | 01332270+3056573 | 14.93 | 22/10/03 | 600 (2) | F4 |
| 182 | 01 33 37.04 | 30 23 23.2 | 1203-0021390 | 8.20 | 7.96 | 01333708+3023213 | 7.58 | 06/09/03 | 480 (2) | A5 |
| 196[6] | 01 33 41.80 | 30 38 48.9 | | | | 01334186+3038491 | 12.61 | 21/10/03 | 7200 (4) | M5 |
| 200[7] | 01 33 43.26 | 30 46 30.7 | 1207-0020534 | 11.58 | 11.13 | 01334337+3046307 | 9.77 | 06/09/03 | 1620 (2) | G5 |
| 204 | 01 33 46.51 | 30 54 32.3 | 1209-0020967 | 11.08 | 10.46 | 01334657+3054308 | 9.91 | 21/10/03 | 1800 (1) | F4 |
| | | | | | | | | 22/10/03 | 3600 (2) | |
| 206 | 01 33 46.66 | 30 54 53.0 | 1209-0020969 | 14.45 | 12.21 | 01334671+3054550 | 11.93 | 21/10/03 | 1800 (1) | K0 |
| | | | | | | | | 22/10/03 | 3600 (2) | |
| 281 | 01 34 26.34 | 30 58 02.7 | 1209-0021391 | 11.15 | 10.48 | 01342664+3058028 | 9.56 | 22/10/03 | 1200 (2) | F8 |
| 297 | 01 34 32.98 | 30 57 54.3 | 1209-0021478 | 13.91 | 12.28 | 01343309+3057538 | 11.89 | 22/10/03 | 2400 (2) | G8 |
| 337 | 01 34 52.99 | 30 28 12.0 | 1204-0021198 | 13.25 | 11.92 | | | 22/10/03 | 1200 (2) | F5 |
| 358 | 01 35 08.29 | 31 02 18.7 | 1210-0021425 | 11.31 | 9.99 | 01350881+3102189 | 13.48 | 18/10/03 | 4500 (3) | galaxy |
| 372 | 01 35 15.42 | 30 55 09.0 | 1209-0021845 | 11.78 | 10.98 | 01351564+3055084 | 10.53 | 22/10/03 | 1200 (2) | F8 |
| 406 | 01 35 51.66 | 30 44 52.3 | 1207-0021551 | 10.04 | 9.38 | 01355164+3044531 | 8.66 | 22/10/03 | 600 (1) | F5 |

* X-ray source numbers from PFH2005 (M 31) and PMH2004 (M 33).
[1] Chandra source s1-74, from Williams et al. (2004).
[2] The adopted spectral type for this object is the average of the spectral types obtained from the two observing runs.
[3] This object is a newly discovered source and it was not included in the PMH2004 catalogue. See Sect. 5.2 for details.
[4] Far off-axis in Chandra observations 1730, not in source list of Grimm et al. (2005).
[5] As explained in Sect. 5.3, the bright USNO-B1 star 1210-0020531 is resolved into two stars on deeper 4 m Mosaic images of M 33, separated by ∼6″ in NNE/SSW direction. The coordinates of these two stars and the corresponding spectral types we derived for them, are given in the two lines following the entry for source 122.
[6] Chandra source CXO J013341.8+303848, from Grimm et al. (2005); no USNO-B1 position, 2MASS position given.
[7] Chandra source CXO J013343.4+304630, from Grimm et al. (2005).

standard spectra have a S/N ranging between 200 and 350, while two have somewhat lower S/N (around 130).

Figure 2 shows six examples of target spectra (black lines), all of foreground stars of different spectral types, that have been flux-normalized for presentation purposes. For comparison, we show in grey the corresponding standard star spectrum (of the same spectral type) shifted in y by an arbitrary amount.

## 4. Spectral classification

Classification of the obtained spectra was achieved via cross-correlation with the 18 standard star spectra.

Each object spectrum was cross-correlated with each standard spectrum, and the height of the corresponding cross-correlation peak (hereafter, ccp) was recorded. These ccp heights

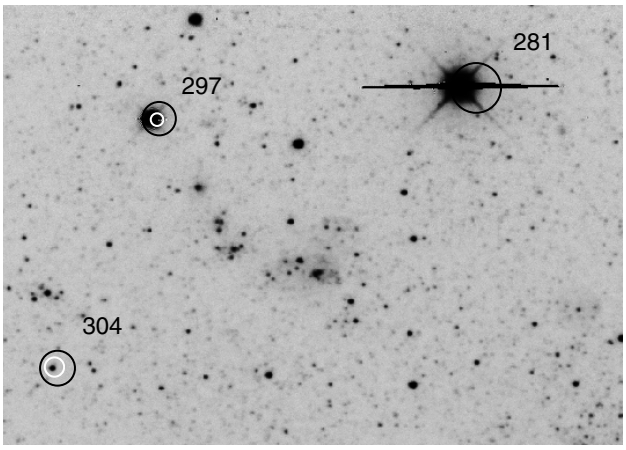


**Fig. 1.** X-ray positions (3-sigma error circles in black) of PMH2004 sources overlaid on the optical image of Massey et al. (2002).The bright stellar counterparts with spectroscopic follow-up of [PMH2004] 297 and 281 are clearly visible. The smaller white circles show the improved positions and errors from the analysis of individual XMM-Newton observations (Misanovic et al. 2006). Note that object 281 was not detected in this latter study. The figure also shows one additional X-ray source in the FoV that was classified as "hard" ([PMH2004] 304).

were plotted as a function of the spectral type of the standard, with the maximum of the curve yielding the adopted spectral type for the object spectrum. Figure 3 shows a typical example of such a plot, for object USNO-B1 1201-0020193. The highest ccp is about 0.9, corresponding to an F5 spectral type. For the entire sample, the highest ccp, on which the spectral classification was based, ranged from 0.7 to 0.95, with most being higher than 0.8.

In some cases there were two ccp (usually for adjoining spectral types in the standard star grid) with comparable heights. For these, we adopted the average spectral type as best representing the spectral class of the object.

As an additional check, we inspected the spectra visually and compared them against those of the standard stars. In very few cases did the spectral type yielded by the cross-correlation method described above have to be modified, after visual inspection. These modifications were always within our estimated error of 0.3 of a spectral type (see below).

The adopted spectral type for each objects is reported in the last column of Table 1.

The accuracy of the spectral classification achieved in this manner depends on the fineness of the grid of standard spectra used and on the signal-to-noise ratio of the cross-correlated spectra. We estimated the accuracy of the spectral classification in the following manner: we treated each standard star as an object spectrum. We cross-correlated it with all of the other standards, and determined its spectral type using the cross-correlation peak curves, as was done for the object spectra. In Fig. 4 we plot the derived spectral type for the standards as a function of the reference spectral type. A least-squares linear fit yields a slope of $0.98 \pm 0.06$ and a scatter of 0.3 in spectral type.

The effect of the S/N on the derived spectral type was estimated by utilizing the individual exposures of various targets. Following the same procedure as for the co-added spectra we derived spectral types and compared them to the spectral types adopted for the co-added spectra. Although the cross-correlation peaks were lower for the lower S/N spectra, the maximum value of the cross-correlation peaks was equally well defined and no differences in spectral classification were noted down to a S/N of about 30. There are two spectra for which the S/N is significantly lower and for these the spectral classification is less accurate (spectral type followed by the symbol "::", in Table 1). Therefore, for almost all of our spectra the accuracy of the spectral classification depends on the fineness of the standard-star grid and is around 0.3 of a spectral type.

For the three spectra obtained in September 2003, the cross-correlation was performed over the common wavelength range between these spectra and the standards (that were obtained in the subsequent observing runs), i.e. over 1000 Å. Despite the shorter wavelength range, the cross-correlation peaks were very high, similar to those obtained for the rest of the spectra. As mentioned earlier, one of the stars ([PMH2004] 3 in M 33) was observed in both wavelength ranges. The spectral classes derived were in excellent agreement (within 0.1 of a spectral type).

## 5. Discussion

All the objects observed, except for [PMH2004] 358 in the direction of M 33 which is a known galaxy (LEDA 5899) and which is discussed separately below, are consistent with being foreground stars, the spectral types of which range from A5 to M5. Figure 5 shows the frequency distribution of the derived spectral types.

In Table 2, we list some of the X-ray properties of the sources (as given in PMH2004 and PFH2005), namely the X-ray flux, $f_x$, the logarithm of the ratio of the X-ray flux to the optical flux, $\log(f_x/f_{opt})$ and the hardness ratios HR1 and HR2.

The fluxes $f_x$ were calculated from the 0.2–4.5 keV XID band. The ratios $\log(f_x/f_{opt})$ were calculated using the formula $\log(f_x/f_{opt}) = \log(f_x) + (B+R)/(2\times2.5) + 5.37$ (Maccacaro et al. 1988) and the USNO-b1 $B$ and $R$ magnitudes given in Table 1. The hardness ratios were derived from the count rates in the energy bands $R_1$ = 0.2–0.5 keV, $R_2$ = 0.5–1.0 keV, and $R_3$ = 1.0–2.0 keV, according to the formulae HR1 = $(R_2 - R_1)/(R_2 + R_1)$ and HR2 = $(R_3 - R_2)/(R_3 + R_2)$, as in PMH2004.

The X-ray fluxes span two orders of magnitude, ranging from 1.5e–15 mW/m$^2$ to 1.47e–13 mW/m$^2$. The values of $\log(f_x/f_{opt})$ range from –5.9 to –2.5, with an average of $-4.2 \pm 0.8$. HR1 takes values between 0.16 and 0.94, with an average of $0.5 \pm 0.2$, while HR2 ranges from –0.93 to 0.32, with an average of $-0.5 \pm 0.3$. There is no clear correlation between any of the X-ray properties listed here and the derived spectral types of the optical counterparts. However, the object with the lowest X-ray to optical flux ratio is the only early type star in the sample (of A type).

All of the objects included in the present study, except for the known galaxy LEDA 5899, satisfy the basic criterion for being foreground stars, i.e. $\log(f_x/f_{opt}) < -1$ (Maccacaro et al. 1988). They also satisfy the additional criterion described in PFH2005, HR2−EHR2 < 0.3 (where EHR2 is the error in the value of HR2, also given in Table 2). In Fig. 6 we plot the hardness ratio HR2 against the X-ray to optical flux ratio [$\log(f_x/f_{opt})$], marking the different spectral classes in different colours. It is clear that all spectral classes in our sample (with enough stars to make the comparison meaningful) occupy the same locus on the $\log(f_x/f_{opt})$-HR2 plane. However, there are three objects, i.e. [PFH2005] 464 in the direction of M 31 and [PMH2004] 206 and [PMH2004] 337 in the direction of M 33, that have hardness ratios too high compared to the rest of the sample (although they do satisfy the previously mentioned criterion for foreground stars). Further inspection of these sources showed that two of them may have overestimated hardness ratios due to their proximity to bright hard sources (see discussion of individual objects

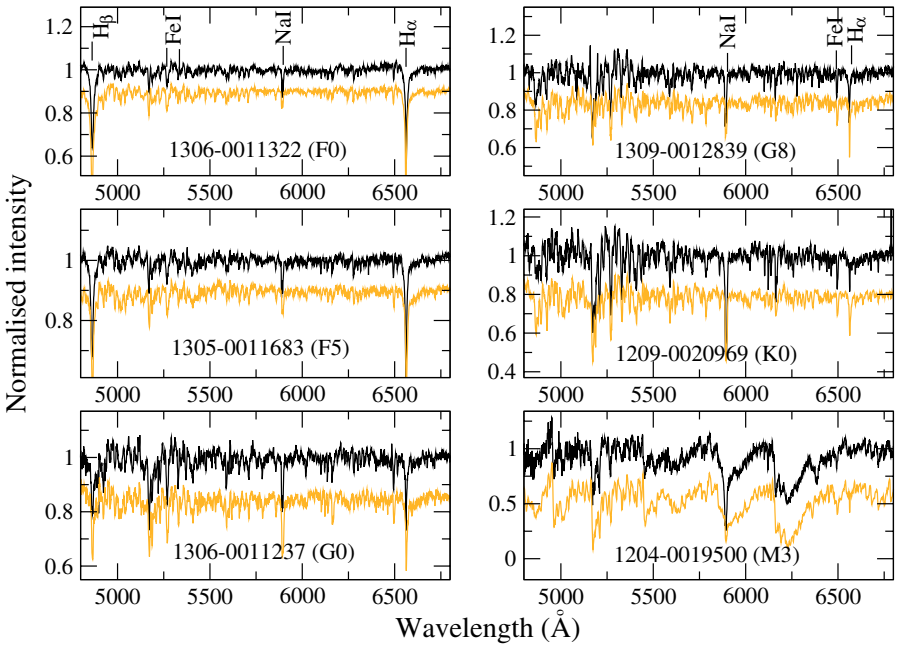


**Fig. 2.** Six examples of spectra (flux normalized) of optical counterparts of X-ray sources in the direction of M 31 and M 33 (black lines). For comparison, we show in grey the corresponding standard star spectrum (of the same spectral type) shifted in $y$ by an arbitrary. The identified lines are $H_\alpha$ (6563 Å), $H_\beta$ (4861 Å), FeI (5270, 5328, 6495 Å) and NaI (5890 Å).

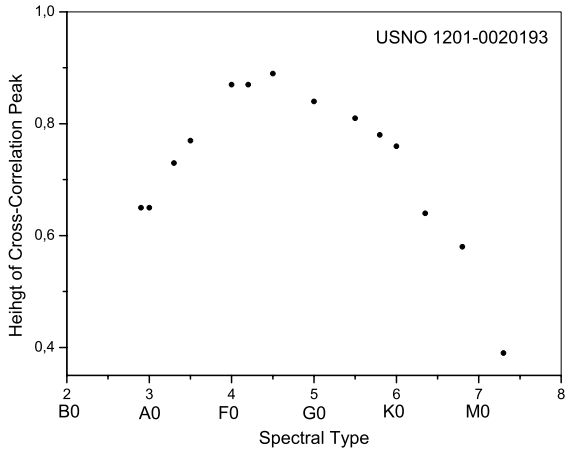


**Fig. 3.** Results of cross-correlation between the spectrum of object USNO-B1 1201-0020193 with each standard star spectrum. On the $x$-axis, the spectral type of the standard star is indicated, while on the $y$-axis the height of the corresponding cross-correlation peak is given.

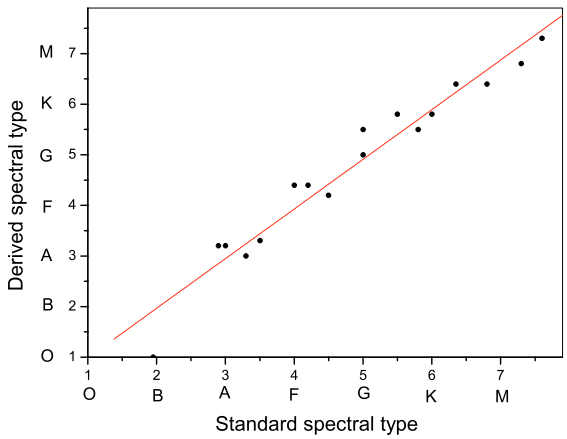


**Fig. 4.** Derived versus standard spectral type for the standard stars.

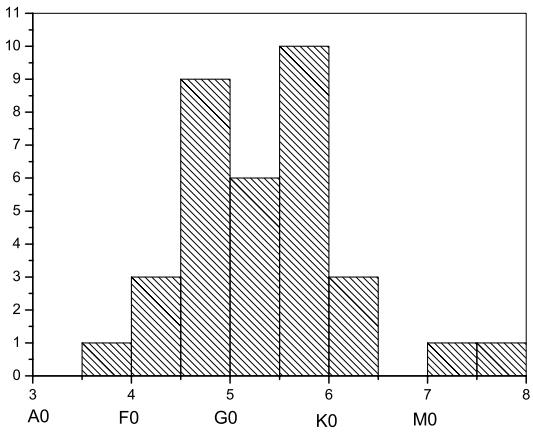


**Fig. 5.** Frequency distribution of spectral types of the observed bright stellar counterparts of X-ray sources in M 31 and M 33.

below). Further discussion of the three sources follows in paragraphs 5.1, 5.5 and 5.7.

### *5.1. [PFH2005] 464, in the M 31 field (USNO-B1 1311-0013521)*

This object has a hardness ratio (HR2) value that is high compared to other stars in the sample with similar X-ray to optical flux ratios (as seen in Fig. 6). The optical spectrum of the star shows no indication of emission lines that might indicate flaring activity. However, the X-ray source itself is quite faint and relatively close to two bright hard sources [PFH2005] 457 ($f_x$ = 3.9e-13 ± 5e-15, HR2 = 0.46 ± 0.01) and [PFH2005] 463 ($f_x$ = 2.7e-13 ± 4e-15, HR2 = 0.81 ± 0.02). Both sources are at a distance of 1.52 arcmin from [PFH2005] 464 and have higher X-ray fluxes by two orders of magnitude. This may disturb the X-ray detection program in the determination of the hard count rate and lead to a harder HR2.

**Table 2.** X-ray properties of the objects of Table 1.

| ID[1] | $f_x$ (mW/m$^2$) | $\log(f_x/f_{opt})$ | HR1 | HR2 |
|---|---|---|---|---|
| | | M 31 | | |
| 26 | 8.3e-15 ± 9e-16 | –3.6 ± 0.1 | 0.47 ± 0.08 | –0.52 ± 0.09 |
| 31 | 2.4e-14 ± 1e-15 | –4.0 ± 0.1 | 0.71 ± 0.04 | –0.60 ± 0.04 |
| 49 | 6.9e-15 ± 7e-16 | –4.2 ± 0.1 | 0.74 ± 0.08 | –0.48 ± 0.07 |
| 59 | 7.0e-15 ± 1e-15 | –4.6 ± 0.2 | 0.39 ± 0.16 | –0.39 ± 0.19 |
| 101 | 6.6e-15 ± 5e-16 | –4.1 ± 0.1 | 0.75 ± 0.05 | –0.69 ± 0.06 |
| 137 | 1.1e-15 ± 4e-16 | –4.8 ± 0.4 | 0.16 ± 0.21 | –0.47 ± 0.27 |
| 168 | 2.9e-14 ± 1e-15 | –3.6 ± 0.1 | 0.68 ± 0.03 | –0.58 ± 0.04 |
| 217 | 2.0e-15 ± 4e-16 | –5.2 ± 0.2 | 0.50 ± 0.12 | –0.93 ± 0.13 |
| 464 | 1.5e-15 ± 5e-16 | –5.1 ± 0.3 | 0.24 ± 0.24 | 0.07 ± 0.22 |
| 479 | 4.9e-15 ± 5e-16 | –4.6 ± 0.1 | 0.68 ± 0.08 | –0.53 ± 0.08 |
| 498 | 2.9e-15 ± 6e-16 | –4.7 ± 0.2 | 0.72 ± 0.17 | –0.60 ± 0.16 |
| 553 | 1.5e-14 ± 1e-15 | –4.0 ± 0.1 | 0.58 ± 0.07 | –0.63 ± 0.08 |
| 615 | 2.1e-15 ± 6e-16 | –4.4 ± 0.3 | 0.30 ± 0.18 | –0.79 ± 0.22 |
| 733 | 2.0e-15 ± 5e-16 | –4.5 ± 0.3 | 0.19 ± 0.23 | –0.33 ± 0.27 |
| | | M 33 | | |
| 3 | 6.33e-15 ± 1.7e-15 | –4.1 ± 0.3 | 0.37 ± 0.21 | –0.64 ± 0.26 |
| 28 | 2.58e-14 ± 2.1e-15 | –3.0 ± 0.1 | 0.44 ± 0.07 | –0.33 ± 0.07 |
| 39 | 6.29e-15 ± 8.7e-16 | –2.6 ± 0.2 | 0.49 ± 0.10 | –0.24 ± 0.11 |
| 54 | 7.51e-15 ± 1.4e-15 | –3.9 ± 0.2 | 0.64 ± 0.15 | –0.75 ± 0.14 |
| 77 | 2.34e-14 ± 3.3e-15 | –3.6 ± 0.2 | 0.67 ± 0.11 | –0.48 ± 0.12 |
| 92 | 2.20e-15 ± 8.2e-16 | –5.2 ± 0.4 | 0.85 ± 0.14 | –0.75 ± 0.18 |
| 122[2] | 4.85e-15 ± 1.7e-15 | –3.0 ± 0.4[2] | 0.94 ± 0.32 | -0.36 ± 0.29 |
| 142 | 2.78e-15 ± 7.8e-16 | –5.5 ± 0.3 | 0.73 ± 0.20 | –0.51 ± 0.22 |
| 182 | 2.94e-15 ± 5.4e-16 | –5.9 ± 0.2 | 0.35 ± 0.13 | –0.54 ± 0.16 |
| 196[3] | 1.49e-14 ± 8.6e-16 | | 0.38 ± 0.05 | –0.65 ± 0.05 |
| 200 | 1.43e-14 ± 9.4e-16 | –3.9 ± 0.1 | 0.61 ± 0.05 | –0.52 ± 0.05 |
| 204 | 5.17e-15 ± 6.5e-16 | –4.6 ± 0.1 | 0.46 ± 0.10 | –0.73 ± 0.11 |
| 206 | 6.05e-15 ± 1.1e-15 | –3.5 ± 0.2 | 0.61 ± 0.32 | 0.32 ± 0.20 |
| 281 | 2.10e-15 ± 5.4e-16 | –5.0 ± 0.3 | 0.31 ± 0.17 | –0.69 ± 0.18 |
| 297 | 7.80e-14 ± 2.2e-15 | –2.5 ± 0.1 | 0.56 ± 0.03 | –0.10 ± 0.03 |
| 337 | 2.09e-14 ± 1.9e-15 | –3.3 ± 0.1 | 0.33 ± 0.12 | 0.30 ± 0.09 |
| 358[4] | 9.51e-15 ± 1.6e-15 | | 0.56 ± 0.20 | –0.14 ± 0.16 |
| 372 | 2.60e-15 ± 7.7e-16 | –4.7 ± 0.3 | 0.80 ± 0.18 | –0.54 ± 0.21 |
| 406 | 1.47e-13 ± 5.3e-15 | –3.6 ± 0.1 | 0.47 ± 0.04 | –0.41 ± 0.03 |

[1] X-ray source, as in Table 1. [2] For the calculation of $\log(f_x/f_{opt})$ for this object we have used the *R* magnitude of the USNO-B1 counterpart given in Table 1, which is most probably a blend of two fainter stars (see Sect. 5.3). Therefore, the derived ratio $\log(f_x/f_{opt})$ should be treated as a lower limit. [3] This source was not identified in the USNO-B1 catalogue (see Sect. 5.4), but only in the 2-MASS catalogue. Thus, there is no estimate of $f_{opt}$, and therefore of $\log(f_x/f_{opt})$ for this object. [4] The published optical and X-ray fluxes do not necessarily correspond to the same contour of the galaxy, thus we did not attempt to calculate $\log(f_x/f_{opt})$ for this object.

### *5.2. Source south-west of [PMH2004] 3 in the M 33 field*

This object, named 3b in Table 1, was not included in the catalogue of X-ray sources of PMH2004. Its position on a EPIC PN CCD boundary, about 30″ south-west of [PMH2004] 3 and far off-axis, prevented its detection by automatic procedures. However, the 0.2–1 keV X-ray image (see smoothed contour overlay in Fig. 7) clearly indicates X-ray emission, most likely originating from the M3 star USNO-B1 1204-0019500 (*R* magnitude 14.66).

The spectrum we obtained for this object is that of an M star.

### *5.3. [PMH2004] 122, in the M 33 field*

This source correlates with the bright USNO-B1 star 1210-0020531. However, inspection of the deeper 4m Mosaic images of M 33 from the Kitt Peak National Observatory archive (from the Local Group Survey of Massey et al. 2002) shows that there are actually two relatively bright stars separated by ∼6″ in NNE/SSW direction which are probably blended into one star in the USNO-B1 catalogue. We have obtained spectra for both stars. They both have G-type spectra, i.e. both stars are compatible with the known X-ray properties of the X-ray source [PMH2004] 122 (see Table 2). Thus, it has not been possible to confirm which of the two stars is the optical counterpart of the X-ray source. More accurate position of the X-ray source would help resolve this question. Unfortunately, the source is outside the FOV of the archival *Chandra* observations.

### *5.4. [PMH2004] 196, in the M 33 field (2MASS01334186+3038491)*

Due to the position of [PMH2004] 196 close to the center of M 33, its optical counterpart was not catalogued in USNO-B1 but only in 2MASS. We therefore give the 2MASS position in Table 1. The optical spectrum identifies it as a late M type star, which shows significant $H_\alpha$ emission (see Fig. 8). The emission line is clearly seen in all four separate exposures obtained for this

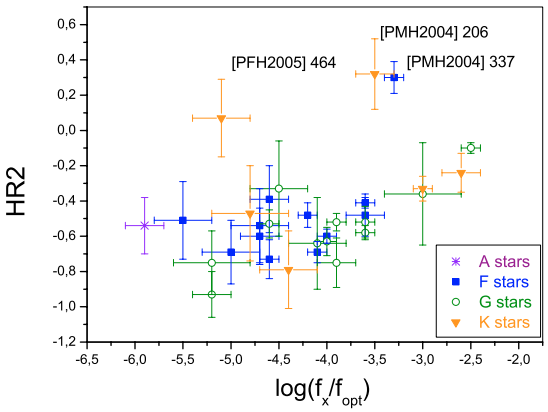


**Fig. 6.** X-ray properties of the observed sample. Different spectral types are marked in different colours.

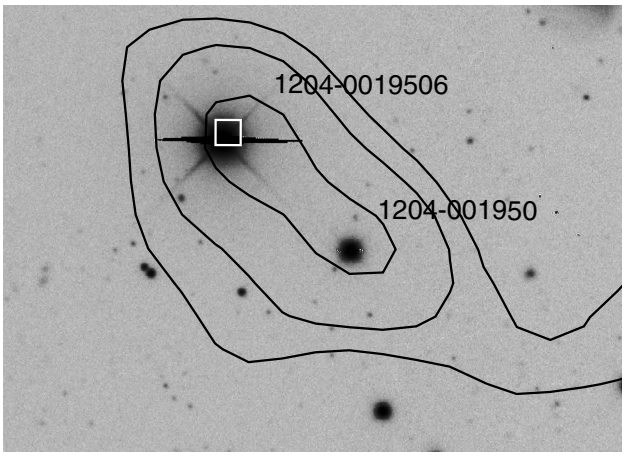


**Fig. 7.** X-ray contours from the (0.2–1.0) keV combined image of PMH2004 overlaid on the optical *R* image of Massey et al. The contours are at levels 3, 4 and $6\times10^{-6}$ cts s$^{-1}$ pixel$^{-1}$, and indicate the position of additional X-ray emission coinciding with the USNO-B1 source 1204-0019500. The position on a pn CCD gap prevented the detection of this emission as an X-ray source. The nearby source [PMH2004] 3 is shown with a box whose size corresponds to the 3 sigma error.

star (the combined spectrum from all four exposures is shown in Fig. 8). The equivalent width of the emission line is estimated to be 5.7 ± 0.3 Å. The presence of Balmer emission lines in late M dwarfs is quite frequent and is linked to variability (e.g. Jaschek & Jaschek 1987). Flare stars are expected to exhibit a late spectral type (typically dwarf M-type) and to present emission in CaII (not included in our spectral range) and in the Balmer lines, during the quiescent phase. The strength of the Balmer emission reaches a maximum during the second phase of a flaring event (i.e. after the first strong continuum phase).

The object displays long-term X-ray variability, changing its average flux by a factor of 6, most likely due to different amounts of flaring activity during the observations. A long term XMM-Newton EPIC light curve is presented in Misanovic et al. (2006, their source 170). The source is also found to be variable in the analysis of Chandra data (Grimm et al. 2005). We analyzed *Chandra* data from the archive to search for flaring. While the source was faint during observation 1730, it showed strong flaring activity during observation 786, when it was found to be brighter on average (see Fig. 9). Although the source is faint in X-rays we managed to produce an XMM-Newton EPIC X-ray spectrum, by combining the counts from three observations. We

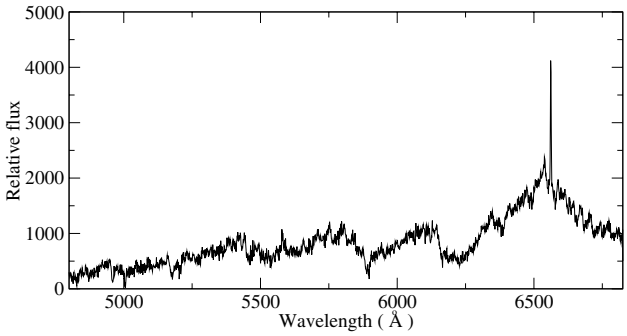


**Fig. 8.** Optical spectrum (not flux normalized) of the optical counterpart of [PMH2004] 196 in M 33, identifying it as a late M star with $H_\alpha$ emission.

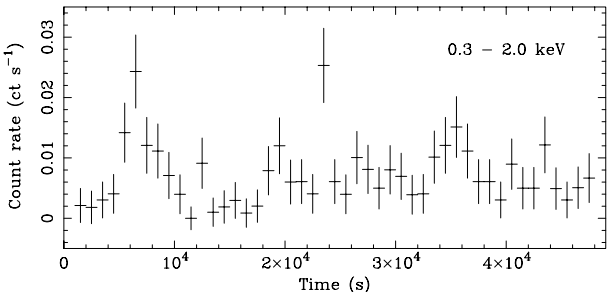


**Fig. 9.** Chandra ACIS S lightcurve of [PMH2004] 196 in M 33 during observation 786 integrated over 1000 s. Time zero corresponds to the start of the observation.

have obtained an acceptable fit to the spectrum for a plasma with *kT* of 2.8 keV. Such a high temperature is expected during flares.

### *5.5. [PMH2004] 206 in the M 33 field (USNO-B1 1209-0020969)*

This is an early-K star which has a somewhat high hardness ratio and it was classified as a possibly hard source by PMH2004. The X-ray flux does not show significant variability within the errors, which are quite high due to the faintness of the source. Moreover, the optical spectrum of the optical counterpart shows no indication of emission lines that might indicate flaring activity. However, the hardness ratio of the source does show some evidence of variability between observations that are spread over three years (Fig. 10). As can be seen in this figure, the source often appears to have a much softer hardness ratio than that given in Table 2 (and plotted in Fig. 6).

There seems to be at least one other early K giant that shows significant coronal activity and some temperature variability (Audard et al. 2004). The authors suggested that most of the coronal heating in that star was contributed by small flares.

### *5.6. [PMH2004] 297, in the M 33 field (USNO-B1 1209-0021478)*

In PMH2004 this object was misidentified as a background elliptical galaxy (object MD 53 in Christian & Schommer 1982). It is actually a stellar source to the North of this galaxy. Indeed, the spectrum is a stellar spectrum of late G-type.

The source displays significant long-term variability in X-rays, changing its flux by a factor of 4. The light curve is presented in Misanovic et al. (2005, their source 253). [PMH2004] 297 is one of the two sources among the objects

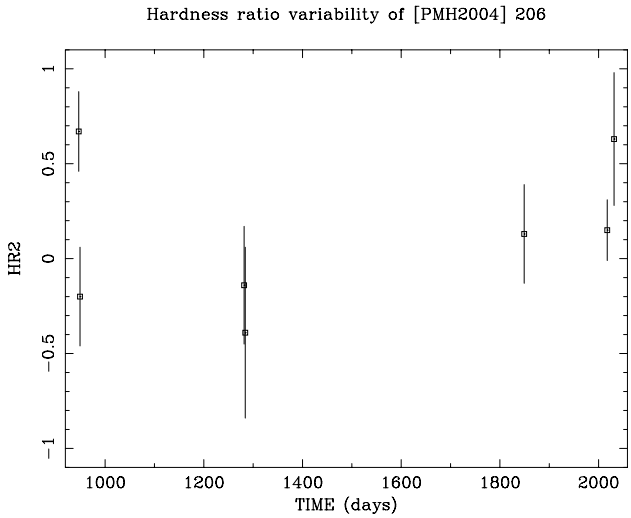


**Fig. 10.** Hardness ratio (HR2 as defined in PMH2004) as a function of epoch of observation for [PMH2004] 206, which corresponds to source 176 in Misanovic et al. (2005). The time is given in days, with the reference day at JD 2 450 814.5.

studied here for which an X-ray spectrum could be produced. Preliminary analysis of the spectrum indicates that it is typical of very active stars (for example see Guedel 2001, 2004). We have obtained an acceptable fit with a combination of two temperature plasmas with $kT$ of 0.8 and 2.3 keV. The high temperature component is most probably produced by flaring or some other type of stellar activity, which may also explain the significant X-ray variability of this source.

### 5.7. [PMH2004] 337, in the M 33 field (USNO-B1 1204-0021198)

This object has a hardness ratio (HR2)[1] value that is too high compared to other stars in the sample with similar X-ray to optical flux ratios. The optical spectrum of the star shows no indication of emission lines that might indicate flaring activity. However, the X-ray source itself is relatively close (0.99 arcmin) to a very bright hard source, [PMH2004] 335 (HR2 = 0.19 ± 0.01), which may disturb the count rate and hardness ratio determination, as it is two orders of magnitude more luminous ($f_x$ = 1.56e − 12 ± 1.6e − 14) than [PMH2004] 337.

### 5.8. [PMH2004] 358, in the M 33 field (LEDA 5899)

This source corresponds to the spiral galaxy LEDA 5899 (CGCG502-114) which is found within the M 33 D25 ellipse and shows a somewhat disturbed appearance. Figure 11 shows images of the galaxy in $U$ and $V$ (top and bottom panel), extracted from the 4m Mosaic images of M 33 from the Kitt Peak National Observatory archive (from the Local Group Survey of Massey et al. 2002). The overlayed circles show the X-ray positions of the source and the corresponding 3 sigma error boxes from PMH2004 (red circle) and Misanovic et al. (2005, yellow circle). The optical spectrum of the galaxy that we obtained here is presented in Fig. 12. Some characteristic lines are marked. Our determined redshift (0.034) agrees within the errors with the value of 0.035 given in Huchra et al. (1999). X-ray variability could not be established for this object, due to lack of sufficient data. The X-ray luminosity of the galaxy in the band (0.2–4.5) keV is found to be 2–3 × $10^{40}$ erg s$^{-1}$, a luminosity typical of normal spiral galaxies (see e.g. Fabbiano et al. 1992).

[1] The source is covered by three individual XMM-Newton observations and detected above the selected threshold in two of them. The HR2 seems to be approximately the same (0.24 and 0.28) in both observations separated by several months.

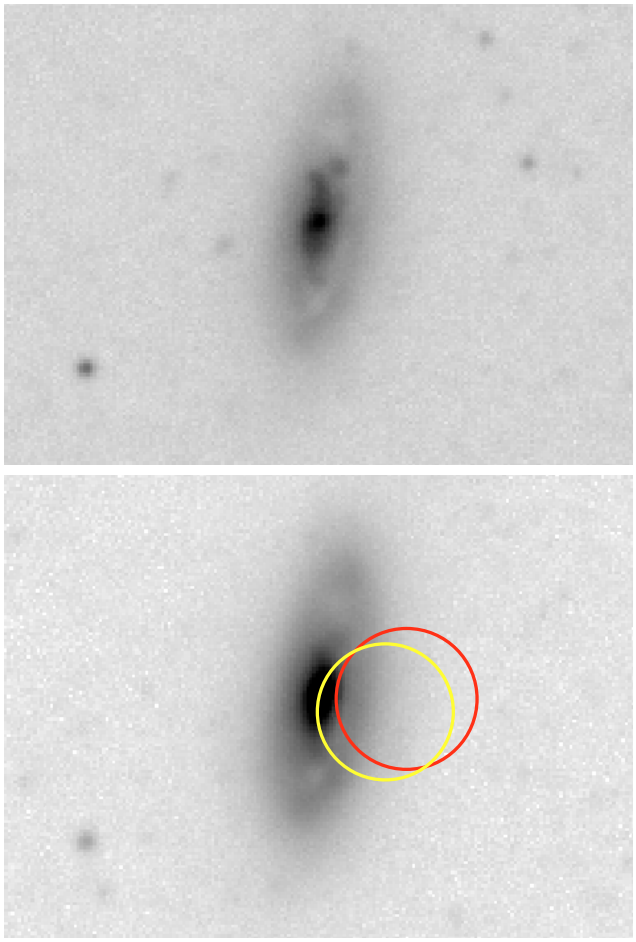

**Fig. 11.** Images of the galaxy LEDA 5899, in $U$ (*top panel*) and $V$ (*bottom panel*). The circles show the X-ray positions of the source and the corresponding 3 sigma error boxes from PMH2004 (bright circle) and Misanovic et al. (2005 dark).

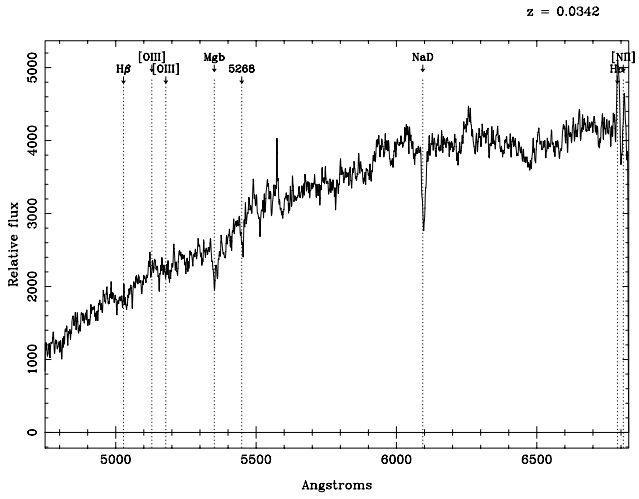


**Fig. 12.** Optical spectrum (not flux normalised) of Galaxy LEDA 5899.

## 6. Summary

We have obtained optical spectra for the 14 brightest optical counterparts of the XMM-Newton source catalogue of the M 31 field (PFH2005) and the 21 brightest counterparts of the XMM-Newton source catalogue of the M 33 field (PMH2004), using the 1.3 m Skinakas telescope in Crete, Greece. All of the M 31 sources and all but one of the M 33 sources are foreground stars, of spectral types between A5 and M 5. One of the M 33 sources (lying within the D25 ellipse) is a background galaxy. The majority of the objects have X-ray hardness ratios and X-ray to optical flux ratios (see Table 2) that are consistent with being a foreground star. One of the stars close to the M 33 center is a late M dwarf with $H_\alpha$ emission, probably a flare star, also displaying strong X-ray variability.

*Acknowledgements.* The authors thank T. Koutentakis and A. Strigachev who helped with the observations at Skinakas Observatory and A. Zezas, for his help in determining the redshift of LEDA 5899. We thank the anonymous referee for very helpful comments.

## References

Audard, M., Telleschi, A., Güdel, M., et al. 2004, ApJ, 617, 531
Christian, C. A., & Schommer, R. A. 1982, ApJ 253, L13
de Vaucouleurs, G., de Vaucouleurs, A., Corwin, H. G., et al. 1991, Third Reference Catalogue of Bright Galaxies (Heidelberg, New York: Springer-Verlag Berlin), Vol. 1–3, XII, 2069, 7
Fabbiano, G., Kim, D.-W., & Trinchieri, G. 1992, ApJS, 80, 531
Grimm, H. J., McDowell, J., Zezas, A., Kim, D.-W., & Fabbiano, G. 2005, ApJS, 161, 271
Guedel, M., Audard, M., Magee, H., et al. 2001, A&A, 365, L336
Guedel, M., Audard, M., Reale, F., Skinner, S. L., & Linsky, J. L. 2004, A&A, 416, 713
Haberl, F., & Pietsch, W. 2001, A&A, 373, 438
Holland, S. 1998, AJ, 115, 1916
Horne, K. 1986, PASP, 98, 609
Huchra, J. P., Vogeley, M. S., & Geller, M. J. 1999, ApJS, 121, 287
Jaschek, C., & Jaschek, M. 1987, in The Classification of Stars (Cambridge: Cambridge University Press)
Maccacaro, T., Gioia, I. M., Wolter, A., Zamorani, G., & Stocke, J. T. 1988, ApJ, 326, 680
Massey, P., Hodge, P. W., Holmes, S., et al. 2002, BAAS, 34, 1272
Misanovic, Z., Pietsch, W., Haberl, F., et al. 2006, A&A, 448, 1247
Monet, D. G., Levine, S. E., Canzian, B., et al. 2003, AJ, 125, 984
Pietsch, W., Ehle, M., Haberl, F., Misanovic, Z., & Trinchieri, G. 2003, Astron. Nachr., 324, 85
Pietsch, W., Misanovic, Z., Haberl, F., et al. 2004, A&A, 426, 11 (PMH2004)
Pietsch, W., Freyberg, M., & Haberl, F. 2005a, A&A, 434, 483 (PFH2005)
Pietsch, W., Fliri, J., Freyberg, M. J., et al. 2005b, A&A, 442, 879
Shortridge, K. 2001, Software in Astronomy, in The Encyclopedia of Astronomy and Astrophysics, ed. P. Murdin (London: Institute of Physics Publishing)
van den Bergh, S. 1991, PASP, 103, 609
Williams, B. F., Garcia, M. R., Kong, A. K. H., et al. 2004, ApJ, 609, 735
Zaritsky, D., Elston, R., & Hill, J. M. 1989, AJ, 97, 97